

Article

Thermodynamic Assessment and Solubility of Ni in LBE Coolants

Pradeep Samui ^{1,2,*} and Renu Agarwal ²¹ Product Development Division, Bhabha Atomic Research Centre (BARC), Mumbai 400085, India² Homi Bhabha National Institute, Bhabha Atomic Research Centre (BARC), Mumbai 400085, India

* Correspondence: pradeepsamui@gmail.com

Abstract: Lead–Bismuth Eutectic (LBE) is a heavy metal liquid alloy used as a coolant for compact high temperature reactors (CHTRs), fast breeder reactor (FBRs) and as a spallation target for ADS. In spite of many advantages due to its thermophysical properties, corrosion towards structural materials remains one of the major issues of LBE. In absence of any oxygen impurity, corrosion in LBE is driven by dissolution processes and the solubility of the main elements of the structural material alloys. Using the CALPHAD method, Thermo-Calc software, a thermodynamic database was developed to assess the interaction between Ni and LBE coolant. The solubilities of Ni in LBE, Bi and Pb liquids have been calculated at different temperatures.

Keywords: LBE; Thermo-Calc; solubility; CALPHAD



Citation: Samui, P.; Agarwal, R. Thermodynamic Assessment and Solubility of Ni in LBE Coolants. *Thermo* **2022**, *2*, 371–382. <https://doi.org/10.3390/thermo2040025>

Academic Editor: Johan Jacquemin

Received: 26 August 2022

Accepted: 15 October 2022

Published: 20 October 2022

Publisher's Note: MDPI stays neutral with regard to jurisdictional claims in published maps and institutional affiliations.



Copyright: © 2022 by the authors. Licensee MDPI, Basel, Switzerland. This article is an open access article distributed under the terms and conditions of the Creative Commons Attribution (CC BY) license (<https://creativecommons.org/licenses/by/4.0/>).

1. Introduction

In the framework of the Generation-IV Nuclear Energy Systems [1] initiative, Pb/LBE is being explored as a coolant for compact high temperature reactors (CHTRs) and fast breeder reactors (FBRs) due to its favourable physical, chemical and nuclear properties. High temperature nuclear reactors have a large potential for sustainably supplying energy for these hydrogen production processes at required high temperature conditions [2]. In Accelerator-driven sub-critical reactor systems (ADS) [3–8], LBE is also considered for coolant and spallation targets [9], with the aim of producing low-cost energy and burning/transmuting the minor actinides and the long-lived radioactive fission product. Other than being inherently safe as they generate power in a subcritical condition, the main advantage of ADS is their application to decrease the radio toxicity load on nature by disposing long-lived radioactive wastes produced in other nuclear reactors. The concept of ADS (frequently called hybrid systems) combines a particle accelerator with a sub-critical core (see Figure 1) [3].

The choice of LBE, as a coolant for fast reactor and as a candidate for spallation target and coolant for ADS, has a number of positive aspects, especially with regard to safety and the strong implications on design simplifications, which provide obvious financial advantages.

However, LBE corrosion of structural materials (clad) is a critical limitation for their use as coolants for nuclear applications; stainless steels are severely damaged when exposed to this heavy liquid at high temperatures. The corrosion behavior of austenitic or martensitic steels in LBE was studied by several authors [10–12]. Most of these studies focused on the oxidation phenomena, directly linked to the oxygen potential imposed during the static or flowing experiments. Compared to corrosion by aqueous media which has been found to be primarily an electro-chemical process, corrosion by liquid metal such as liquid lead and lead–bismuth alloy is a physical or physico-chemical process involving dissolution of material constituents, transportation in the two phases (liquid and solid) and reactions between corrosion products and impurities [13–15]. It has been reported that the corrosion by liquid metals/alloys can change the microstructure, composition, and

surface morphology of the structural materials, which in turn affects the mechanical and physical properties of the structural materials, leading to system failure [15–27]. The rate of dissolution of the structural materials remains of major importance too when considering the resistance of the alloys because it drives the LBE chemistry [10,11]. To understand the clad–coolant interaction, i.e., the interaction of stainless-steel structural materials with Bi-Pb, it is important to know the thermo-physical properties of alloys/compounds formed by interaction of Pb and Bi with all major elemental component of steel, i.e., Fe, Cr and Ni. Among Fe, Cr and Ni, the former two elements, Fe and Cr, have very slight solubilities in Pb/Bi, whereas the solubility of Ni in Pb/Bi is maximum. Nickel also makes two intermetallic compounds with Bi. However, the lack of reliable thermodynamic data (solubility limit and chemical activity) in such complex systems makes it difficult to explain the non-equilibrium behavior and the interactions observed in experimental studies on LBE [10–14]. Unfortunately, computation based on the CALPHAD approach is not available in the literature for the interactions between the Bi-Pb heavy metal coolant and the major constituting elements of the alloys: Fe-Cr-Ni. Nickel is the main component of stainless-steel structural material that shows strong interactions with lead, bismuth or LBE coolants. Therefore, in this study, assessment of the Bi-Ni-Pb ternary system using only binary interaction parameters was carried out and solubility limits of nickel in Bi, Pb and LBE coolants at different temperatures was calculated.

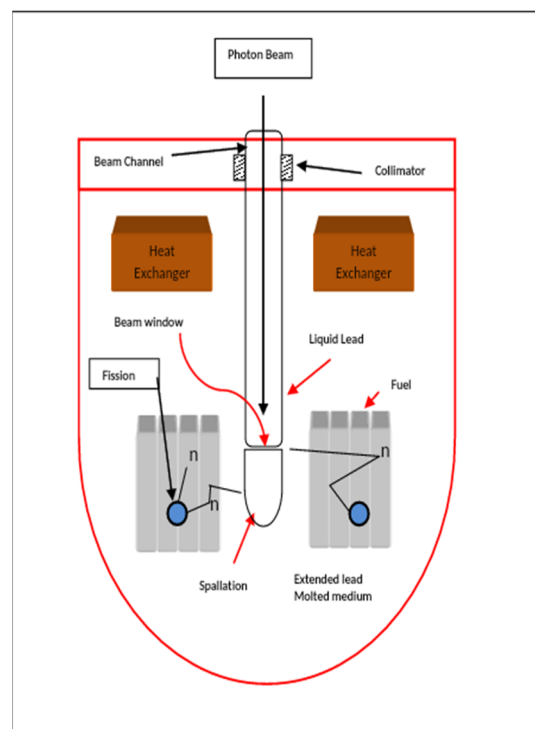


Figure 1. Schematic of ADS reactor system.

2. Thermodynamic Modeling

The temperature dependencies of the molar free energies for the pure elements are described in the following form according to ref [28]:

$$G_i^0(T) - H_i^{SER} = A_i + B_iT + C_iT \ln T + D_iT^2 + E_i/T + F_iT^3 + I_iT^4 + J_iT^7 + K_iT^9 + \Delta G_{mag}(T) \quad (1)$$

where, $G_i^0(T)$ is the Gibbs energy of a pure element 'i' at temperature T , H_i^{SER} represents the enthalpy of the pure element 'i' in its stable state at the standard temperature 298.15 K and pressure 1 bar; T is temperature and $\Delta G_{mag}(T)$ is the magnetic term. Values of coefficients A , B , C and K for the lattice stabilities of the pure elements were taken from Pure4 database in

Thermocalc [29]. The molar Gibbs energy for a binary phase is expressed by the following equation:

$${}^oG_m^\phi - \sum_{i=A,B} x_i^\phi {}^oH_i^{SER}(298.15 \text{ K}) = \sum_{i=A,B} x_i^\phi \left\{ {}^oG_i^\phi - {}^oH_i^{SER}(298.15 \text{ K}) \right\} + RT \sum_{i=A,B} x_i^\phi \ln(x_i^\phi) + G^{\phi,xs} \quad (2)$$

where, x_i denotes the atomic fraction of the 'i' element. 'R' is the universal gas constant. The excess Gibbs energy, $G^{\phi,xs}$, of a binary solution is expressed by the Redlich–Kister polynomial equation [30].

$$G^{\phi,xs} = x_i^\phi x_j^\phi \sum_{v=1}^n {}^vL_{i,j} (x_i^\phi - x_j^\phi)^v \quad (3)$$

where, the interaction parameters, $L_{i,j}^\phi$ (with $v = 0,1$) can be temperature dependent in the Redlich–Kister power series, are expressed by:

$${}^vL_{i,j}^\phi = \alpha + \beta T \quad (4)$$

where, α and β are the adjustable interaction parameters refined to replicate the experimental data. The ternary Ni-Bi-Pb assessment is based on extrapolations of the most important binary sub systems: the Bi-Pb, Bi-Ni and Ni-Pb systems. The thermodynamic assessments of the Bi-Pb and Bi-Ni binary systems were performed in this study. The third binary Ni-Pb system was taken from the literature.

2.1. Thermodynamic Assessment of Bi-Pb System

The use of LBE as a coolant in nuclear systems makes it necessary to improve interpretation of the origin of the low temperature liquid phase. In this binary system, the liquid comes from the eutectic reaction (Liquid \leftrightarrow Bi-Rhombo + BiPb_{3±x}), calculated at 399 K. At this temperature, rhombohedral Bi (Bi-Rhombo), liquid and hexagonal close-packed intermetallic phase (BiPb_{3±x}) are in equilibrium. Therefore, the Bi-Pb system has only one non-stoichiometric compound, BiPb_{3±x}. The maximum solubility of Bi in Pb-FCC is ~78 at% Pb at 457 K [31,32]. The solubility of Pb in Bi-Rhombo is negligible [31]. The phase boundary of BiPb_{3±x} was based on the studies carried out by Wolt et al. [33] (resistivity measurement), Predel et al. [34] (thermal analysis, microscopy, resistivity and X-ray) and Hoff et al. [35] (X-ray and resistivity measurement). The emphasis is given on the Predel et al. [34] and present thermodynamic calculations. The data of obtained by resistivity measurements sometimes appeared to be overestimated. The solubility limit of the Bi in Pb-FCC phase is a combination of X-ray data of Hay et al. [36], the results of Predel et al. [34] and the data of Wolt et al. [33] and Hoff et al. [35], and the phase diagram of Yoon et al. [32]. It is evident from Figure 2, that the result of resistivity measurement is too high as compared to other data. The reason behind this is the poor resolution in the measurement and systematic error associated with non-ideal nature of measurement. However, the time of equilibration of BiPb_{3±x} phase is also important when below a temperature of 200 °C. Complete homogenization of alloys into that BiPb_{3±x} phase may not have accomplished due to low diffusion rate. It can take a long time to determine the phase boundary at a lower temperature. The phase diagram was optimized by Boa et al. [31] and Yoon et al. [32]. It was found that the optimized parameters of Boa et al. and Yoon et al. did not have any excess heat capacity coefficients for BiPb_{3±x}. The heat capacity, enthalpy of formation of BiPb₃ and the enthalpy of mixing of liquid solution were measured by the authors [37,38]. Using these important thermodynamic data along with phase-diagram and Gibbs energy data available in the literature [32–36,39,40], the optimization of interaction parameters of the system was performed with the help of Thermocalc software based on CALPHAD approach. The calculated phase diagram of the Bi-Pb system and all experimental phase diagram data [32–36,39,40], which are used in the present optimization, are shown in the Figure 2. The phase boundaries calculated from previous optimizations reported in the literature are also drawn in the Figure 2 [30,31]. It is seen that the present assessment is in reasonable agreement with previously reported assessments and experimental data. All

invariant reactions in the Bi-Pb system are summarized in Table 1, with the calculated data from previous assessment. A complete set of the present assessed thermodynamic descriptions of this system is given in Table 2.

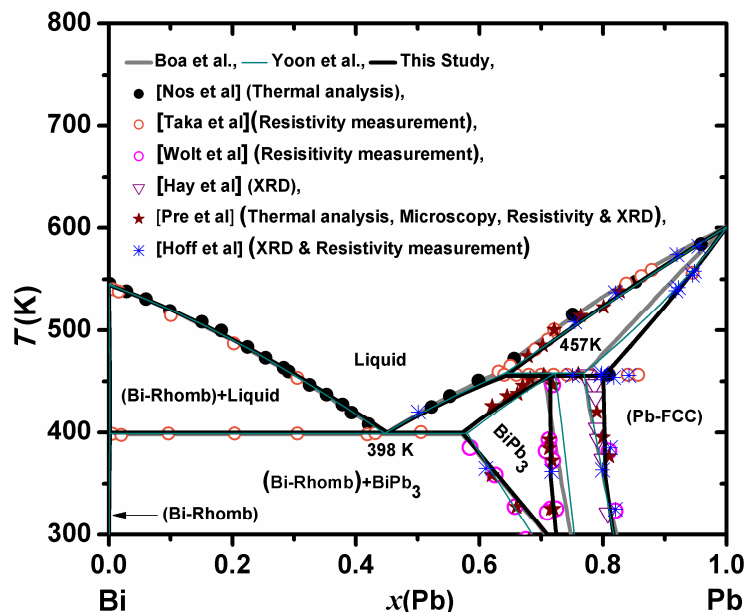


Figure 2. Calculated phase diagram of Bi-Pb system with experimental data (Wolt et al. [33], Predel et al. [34], Hoff et al. [35], Hay et al. [36], Nos et al. [39], Taka et al. [40]).

Table 1. Comparison of invariants in Bi-Pb system between previous assessment and this study.

Reaction	Type	T/K	Composition, $x(\text{Pb})$			References
L + Pb-FCC = BiPb ₃	Peritectic	457.5	0.62	0.78	0.719	[31]
		457	0.64	0.769	0.72	[32]
		457	0.63	0.819	0.719	This Study
L = BiPb ₃ + (Bi-Rhomb)	Eutectic	398.5	0.446	0.58	0.005	[31]
		398.5	0.446	0.58	0.005	[32]
		399	0.446	0.58	0.005	This Study

Table 2. Assessed parameters for the Bi-Ni-Pb ternary system.

Phase and Model	Thermodynamic Parameters
LIQUID [Bi,Ni,Pb] ₁	${}^0L_{\text{Bi,Ni}}^{\text{Liq}} = -19992.628 + 99.11350 \times T - 10.0574 \times T \times \ln(T)$
	${}^1L_{\text{Bi,Ni}}^{\text{Liq}} = 1.2944 - 191.9533 \times T + 25.5048 \times T \times \ln(T)$
	${}^2L_{\text{Bi,Ni}}^{\text{Liq}} = 12521.6048 - 1.5602 \times T$
	${}^0L_{\text{Bi,Pb}}^{\text{Liq}} = -5050.202 + 1.85 \times T$
	${}^1L_{\text{Bi,Pb}}^{\text{Liq}} = -1050.01 + 1.18 \times T$
	${}^0L_{\text{Ni,Pb}}^{\text{Liq}} = +31532.257 - 2.42 \times T$
	${}^1L_{\text{Ni,Pb}}^{\text{Liq}} = +10459.949 - 2.49 \times T$
	${}^2L_{\text{Ni,Pb}}^{\text{Liq}} = -10927.18 + 7.952 \times T$
	${}^3L_{\text{Ni,Pb}}^{\text{Liq}} = -3732.467 - 0.109 \times T$
BiPb ₃ [Bi, Pb] ₁	${}^0L_{\text{Bi,Pb}}^{\text{BiPb3}} = -3450.04 + 9.781 \times T - 2.5001 \times T \times \ln(T) - 496987.08/T$
	${}^1L_{\text{Bi,Pb}}^{\text{BiPb3}} = -1.801 \times T$
Pb-FCC [Bi, Pb] ₁	${}^0L_{\text{Bi,Pb}}^{\text{Pb-FCC}} = -3550.05 + 1.11 \times T$

Table 2. Cont.

Phase and Model	Thermodynamic Parameters
Bi-Rhomb [Bi, Pb] ₁	${}^0L_{Bi,Pb}^{Bi-Rhomb} = 3461.56$
Bi ₃ Ni [Bi] ₃ [Ni] ₁	${}^0G_{Bi,Ni}^{Bi_3Ni} = -2450.002 + 9.1195 \times T - 1.9 \times T \times \ln(T) + 0.75G^{Bi-rhomb} + 0.25G^{Ni-FCC}$
BiNi[Bi] _{0.3334} [Ni] _{0.3333} [Bi,Va] _{0.3333}	${}^0G_{Bi,Ni}^{BiNi} = 0.667G^{Bi-rhomb} + 0.333G^{Ni-FCC}$ ${}^0G_{Bi,Ni,Va}^{BiNi} = -4250 + 13.37 \times T - 1.8 \times T \times \ln(T) + 0.333G^{Bi-rhomb} + 0.333G^{Ni-FCC}$ ${}^0L_{Bi,Ni,Va}^{BiNi} = -1647 + 1.434 \times T$
Ni-FCC [Bi,Ni,Pb] ₁	${}^0L_{Bi,Ni}^{Ni-FCC} = -20000 + 12.5 \times T$ ${}^0L_{Ni,Pb}^{Ni-FCC} = +29980 + 0.59 \times T$ ${}^1L_{Ni,Pb}^{Ni-FCC} = -20000 + 25 \times T$

2.2. Thermodynamic Assessment of Bi-Ni System

There are two intermetallic compounds, Bi₃Ni and BiNi, in the Bi-Ni system. The solubility of Bi in Ni-FCC is very limited. No Ni solubility is considered in the rhombohedral structure of Bi. The Bi₃Ni phase is stoichiometric while BiNi exhibits a narrow composition range towards the Bi-rich domain. Some publications indicate a narrow non-stoichiometric region for both compounds. However, due to lack of experimental data on non-stoichiometric range of stability of Bi₃Ni, only BiNi is assumed to be non-stoichiometric in the present assessment calculations. In light of new calorimetric data of the system; acquired by authors [41,42], the Bi-Ni system was re-optimized. The thermodynamic assessment was carried out by optimizing experimental phase diagram and thermodynamic data available in the literature [43–47] and our experimental data of (i) heat capacity, (ii) enthalpy increment, (iii) enthalpy of formation of compounds and (iv) enthalpy of mixing of liquid phase [41,42]. The calculated phase diagram of the Bi-Ni is shown in Figure 3. It is seen that the calculated results are in reasonable agreement with previous assessments [43,48] as well as experimental phase diagram data [43–47]. A complete set of the present assessed thermodynamic descriptions of this system is given in Table 2.

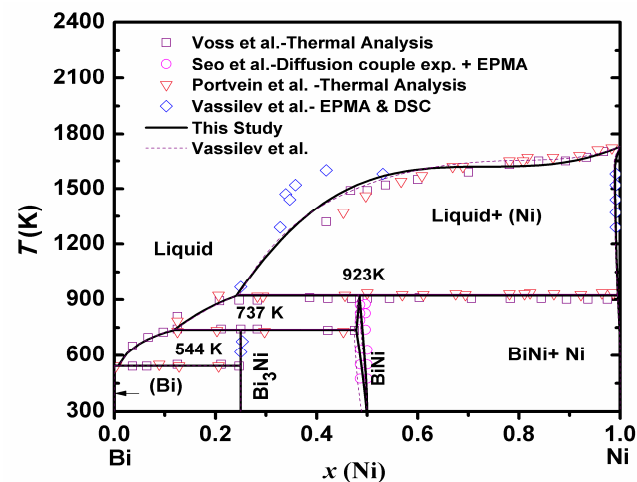


Figure 3. Calculated phase diagram of Bi-Ni system with experimental phase diagram data point from the literature (Vassilev et al. [43], Voss et al. [44], Seo et al. [45], Portvein et al. [46]).

All invariant reactions in the Bi-Ni system are summarized in Table 3, along with the calculated data from previous assessments for comparison.

Table 3. Comparisons of invariants in Bi-Ni system.

Reaction	Type	T/K	Composition, $x(\text{Ni})$			References
BiNi = (Ni-FCC) + Liq	Peritectic	920.7	0.759	0.515	0.00485	[43]
		919.0	0.762	0.510	0.022	[48]
		921.0	0.76	0.517	0.005	This work
Bi ₃ Ni = BiNi + Liq	Peritectic	737.2	0.881	0.75	0.52	[43]
		738.0	0.877	0.75	0.515	[48]
		737.5	0.878	0.75	0.52	This work
Liq = Bi ₃ Ni + (Bi-Rhomb)	Eutectic	542.8	0.75	0.993	1.0	[43]
		543.0	0.75	0.993	1.0	[48]
		543	0.75	0.991	1.0	This work

3. Interaction of Pb/Bi with Ni

As discussed earlier, nickel is one of the main components of stainless-steel structural material that will show strong interactions with lead, bismuth or LBE coolants. Therefore, it is important to assess this ternary system and find out solubility limits of nickel in these coolants at different temperatures. It is also of great significance to know what solid phases may precipitate out at different temperatures. Precipitation of a compound in a coolant can be detrimental to its performance as it can be carried to different parts and accumulate in certain sensitive areas, which can obstruct the smooth flow of coolant, thus causing local heating and swelling. In addition to this, these interactions thin the clad due to chemical abrasion. In extreme conditions, this can cause a burst of coolant channels and an accidental loss of coolant. In addition, thermodynamic properties such as heat capacities, enthalpies of formations and enthalpies of transitions of these precipitating phases at different temperature can affect the thermal performance of the coolant, which goes through different thermal conditions during the heating and cooling of the reactor. Depending on its location, even in an operating nuclear reactor, coolant can be exposed to very different temperatures.

- Therefore, to understand different phases formed by the interaction of Pb/Bi and Ni, the Bi-Ni-Pb ternary was computed. As discussed in Sections 2.1 and 2.2, respectively, Bi-Pb and Bi-Ni binaries of this ternary were re-optimized using the experimental data acquired during this work. The third binary required for computing the Bi-Ni-Pb ternary is Ni-Pb. This binary system does not have any intermetallic compound and its thermodynamic assessment can be reliably obtained from a thermodynamic description of unary elements and the binary phase diagram data available in the literature. Therefore, no new experimental data was acquired for this system. The phase description for Ni-Pb system was taken from Ghosh et al. [49]. The modeling by Ghosh et al. considers numerous sets of phase diagram data and thermodynamic information from the literature [44,46,50–53]. For the sake of clarity, the Ni-Pb system is shown in the Figure 5. The Ni-Pb binary has a liquid phase miscibility gap, does not have any intermetallic compound and the FCC-Ni phase dissolves a small amount of Pb. In the absence of experimental thermodynamic or phase diagram data for the Bi-Ni-Pb ternary, computation of this system was based on the following assumptions:
- As crystal structures of all the intermetallic compounds, Bi₃Ni, BiNi and BiPb₃, are quite different, they were assumed to be present as pure binary compounds in the ternary system.
- The liquid phase and end member solubilities were modeled by using only binary interaction parameters
- In absence of any experimental data to indicate the presence of stable ternary compounds, no new ternary phase was considered.
- To understand Ni interaction with LBE at different temperatures, a pseudo binary diagram along the isopleth LBE-Ni was computed (Figure 4). As there was no available experimental data in the literature on this ternary system, it was decided to study

transition temperatures of this pseudo-binary system, using DTA. For this purpose, alloys with different compositions of Ni in LBE ($0.38 < x(\text{Ni}) < 0.46$) were prepared. The alloys were prepared by melting desired ratios of lead, bismuth and a fine powder of nickel metal. The liquid mixture was slowly cooled in a furnace to ambient temperature. DTA analysis of these alloys was carried out using an indigenously fabricated DTA instrument. The temperatures of phase transitions were obtained from the extrapolated peak onset temperature during heating of alloys at 5K/min. The present DTA results of selected compositions are plotted in Figure 4 of pseudo-binary phase diagram of LBE-Ni system. Our experimental data shows reasonable agreement with the computed pseudo binary diagram. It proves that the above listed assumptions used for the computation of the ternary system were acceptable. Hence, inferences based on the ternary database, generated using binary interactions, should be reliable.

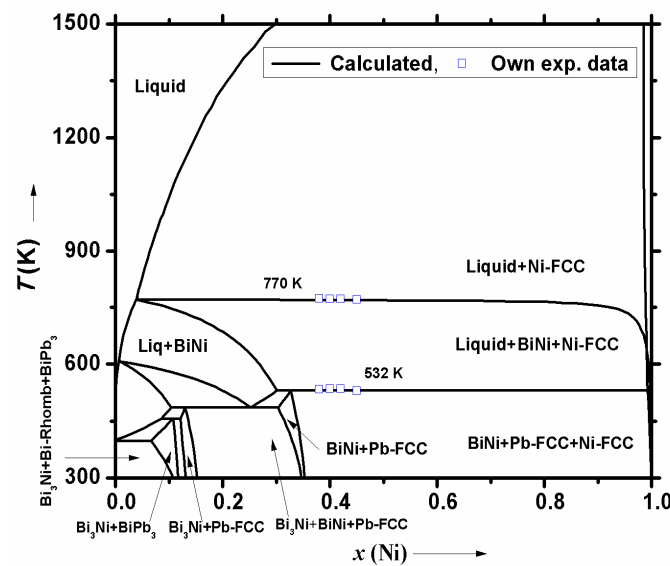


Figure 4. Calculated isopleth for pseudo binary of LBE-Ni ($\text{Bi}_{0.55}\text{Pb}_{0.45}\text{-Ni}$) and comparison with DTA results.

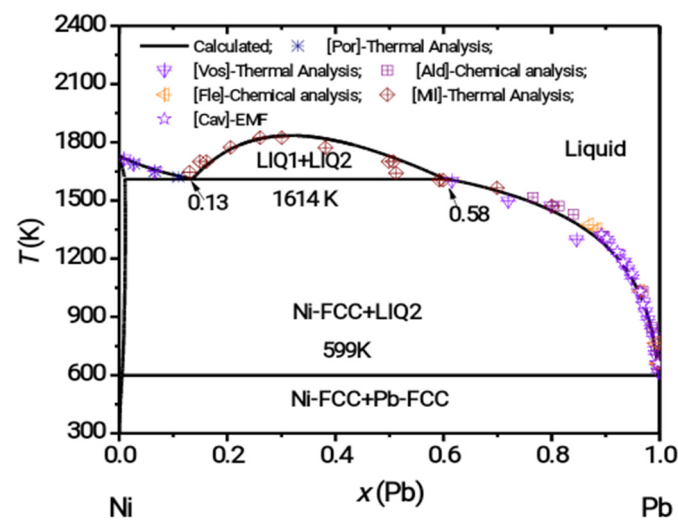


Figure 5. Calculated phase diagram of Ni-Pb system and experimental data from literature ([Vos] [44], [Por] [46], [Ald] [50], [Fle] [51], [Mi] [52], [Cav] [53]).

The pseudo binary phase diagram of LBE-Ni given in Figure 4 has generic similarity to Bi-Ni phase diagram. This is mainly due to the presence of high melting nickel metal in both the diagrams and low temperature decomposition of BiPb_3 compound. However, the

prominent difference in these two diagrams is that the solubility limit of nickel in bismuth liquid is much higher than in LBE, as the liquid of Bi-Ni is richer in nickel than of LBE-Ni system. For example, solubility of Ni in bismuth liquid at 600 K is 2 at.% Ni and in LBE is 0.6 at.%, whereas at 770 K, 14 at.% Ni dissolve in Bi(l) and 2.6 at.% Ni in LBE and at 1273 K, 35 at.% Ni dissolve in Bi(l) and 16 at.% Ni in LBE. The latter temperature (1273 K) is seen by the coolant of High Temperature Compact Reactor (CHTR) [54]. At temperatures below 770 K, longer erosion of Ni by LBE will result in formation of BiNi/Bi₃Ni compound. At room temperature, LBE has the BiPb₃ compound in equilibrium with ‘Bi-Rhomb’. Due to the interaction of LBE with ‘Ni’ at high temperatures, the Bi₃Ni compound may also become precipitated. At ambient temperature, the Pb-FCC phase will not be observed as it interacts with bismuth to form BiPb₃. Therefore, bismuth metal will react with both Ni and lead and form compounds, BiPb₃ and Bi₃Ni. During the cooling of liquid coolant, significant heat will be generated due to enthalpy of fusion of Pb/Bi and formation of intermetallic compounds, BiPb₃, Bi₃Ni and BiNi. Heat capacity of these intermetallic compounds is slightly higher than that of pure elements [38,41]. Therefore, coolant temperature will decrease at a slower rate in presence of intermetallic compounds. A similar effect will be seen when heating coolant to liquid phase, as coolant that contains these compounds will need more heat to melt completely.

A complete set of the presently assessed thermodynamic descriptions of this ternary system is given in Table 2.

4. Solubility of Nickel in LBE/Bi/Pb

As discussed earlier, due to the relatively high solubility of the major alloying components of steel, LBE is severely corrosive to steel, especially at high temperatures (>1000 K). As previously mentioned, precipitation at cold walls is catastrophic because severe precipitation may lead to the clogging of piping and degradation of heat transfer. During a long period of operation, especially at high temperature, corrosion of structural material can change its composition, microstructure and strength, which can be detrimental to its safe operation. Hence, it is important to know the solubility of components of steel in pure liquid Pb, Bi and LBE. Solubility limits of Ni were calculated in Pb(l), Bi(l) and LBE(l). The calculations were carried out using the interaction parameters given in Table 2. Calculated and experimentally determined solubilities of Ni in Pb, Bi and LBE are compared in Figure 6.

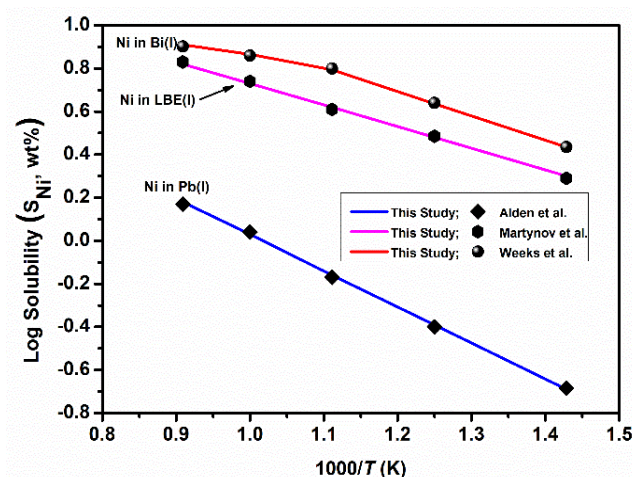


Figure 6. Solubility of Ni in liquid Pb, Bi and LBE and compared with experimental data (Alden et al. [50], Martynov et al. [55], Weeks et al. [56]).

As can be seen in Figure 6, there is an excellent agreement between experimental data reported in the literature [50,55,56] and values calculated from the present thermodynamic assessment of this ternary system. Solubility of Ni in LBE is more than that in Lead. Among major steel components, solubility of Ni is highest in Bi, LBE or Pb. At most of the reactor

operation temperatures, Bi is not a suitable coolant as it is more corrosive than Pb and LBE. The corrosion process is mainly driven by dissolution of the alloying element in the coolant [57]. The key parameters to model such a process is the solubility and chemical activity of the main elements of the alloy. According to Figure 6, the solubility of Ni in Bi(*l*) is the highest as compared to Pb and LBE. At the same time, pure Bi has highest chemical activity to react with Ni in steel and it has more potential to penetrate through grain boundaries/pores of the structural materials as compared to LBE, which results in more corrosiveness. In the absence of Ni, LBE is a better coolant than Bi, as it dissolves a lowest amount of Fe/Cr. Solubility of Fe, Cr and Ni in Pb(*l*), LBE(*l*) and Bi(*l*) is tabulated in the Table 4. This indicates that the solubility of Fe and Cr is approximately 2–3 order of magnitude less than that of Ni in the temperature range 700–1100 K. Pb(*l*) has lowest power to dissolve Fe and Cr.

Table 4. Solubility $\{\log_{10} S \text{ (wt\%)}\}$ of Fe and Cr in liquid Pb, LBE and Bi.

Temp. T(K)	Fe Solubility			Cr Solubility			Ni Solubility		
	Pb(<i>l</i>)	LBE(<i>l</i>)	Bi(<i>l</i>)	Pb(<i>l</i>)	LBE(<i>l</i>)	Bi(<i>l</i>)	Pb(<i>l</i>)	LBE(<i>l</i>)	Bi(<i>l</i>)
600	−8.03	−6.76	−5.78	−8.86	−5.36	−5.07	−1.08	−0.6	−0.24
700	−6.78	−5.71	−4.84	−7.27	−4.64	−4.20	−0.69	0.30	0.41
800	−5.85	−4.93	−4.14	−6.09	−4.09	−3.57	−0.39	0.48	0.69
900	−5.13	−4.32	−3.59	−5.16	−3.67	−3.06	−0.16	0.62	0.90
1000	−4.54	−3.83	−3.16	−4.42	−3.33	−2.66	0.03	0.73	0.87
1100	−4.07	−3.43	−2.80	−3.81	−3.05	−2.33	0.18	0.82	0.91
1200	−3.67	−3.09	−2.50	−3.32	−2.82	−2.06	0.31	0.90	0.95

The solid solubility of Ni in Pb is negligible at 598 K. The solubility of nickel is 0.53 at.% at 645 K and 18.63 at.% at 1473 K [50]. The solubility of Ni in liquid Bi has three domains due to formation of an intermetallic. The first domain of temperature range where liquid and Bi₃Ni are in equilibrium is 543–742 K and the second is 742–917 K. Beyond 918 K, the liquid and Ni-FCC are in equilibrium. The Ni solubility given in Table 4 are in accordance with these three domains and are in excellent agreement with Gosse et al. [58]. The solubility of Ni in LBE is much higher than that of Fe and Cr, indicating that Ni content in steels used as a container of LBE needs to be reduced or the steel needs to be protected to increase the corrosion resistance. The solubility of Fe, Cr and Ni in LBE is always greater than that in liquid lead, as is shown in Table 4. However, the pure lead melting point is higher than that of LBE and a higher operation temperature is needed if liquid lead is to be used as a nuclear coolant.

5. Mechanisms of Liquid Metal/Alloy Corrosion

Degradation of steels in liquid Bi, Pb or LBE occurs mainly through dissolution of steel components into the liquid under static flow. The key driving force for liquid metal corrosion is the chemical potential and activity of the element for dissolution in contact with the liquids [58]. The rate of dissolution is governed by the composition of solid metal and liquid media, the area of the solid surface exposed, the flow rate as well as the surface morphology and impurity content. The local corrosion occurs mainly due to intergranular penetration of liquid through the solid meeting, due to the presence of pore defects. During non-static condition of liquid coolant, the flow assisted or erosion corrosion are found to occur. Factors affecting the corrosion rate are distributed into three groups in terms of chemical, metallurgical, and technological factors. We will discuss chemical factor in this paper. The chemical factors include the chemical composition of the liquid metal and its impurity contents, the flowing conditions (the pressure and the flow velocity), the temperature and its profile, the exposure time, etc.

The chemical composition of liquid is changed due to dissolution and formation of compound. Therefore, the dissolution plays a significant role in corrosion phenomena. In this study, we have seen that among Fe, Cr and Ni, the solubility/dissolution of Fe and Cr

is less as compared to Ni, as shown in Table 4. In LBE coolant, it also forms an intermetallic compound.

To tackle corrosion problems of lead based liquid coolants, nickel-free steel alloys are being investigated. In addition, some corrosion inhibitors, e.g., oxygen, Zr or Ti, and alloying elements, e.g., aluminium and molybdenum, are being tested.

6. Conclusions

Analysis by CALPHAD method and experimental DTA techniques of Bi-Ni-Pb system were carried out. Using the CALPHAD method, a thermodynamic database was developed to assess the interaction between Ni alloys and LBE. Bi-Pb and Bi-Ni systems were reassessed, based on our experimental data. LBE-Ni pseudo-binary phase diagram was calculated from a ternary database. DTA analysis of LBE-Ni in the present work was carried out to experimentally confirm the invariant temperature computed from the ternary database. This work shows that the solubility of Ni is higher in Bi than in Pb or LBE. The experimental solubility results from the literature and the thermodynamic calculations. These calculations may provide a better thermodynamic description of the dissolution phenomena in the Bi-Ni-Pb system when corrosion mechanisms are mostly assisted by dissolution or precipitation processes.

Author Contributions: Conceptualization, P.S.; methodology, P.S.; software, P.S.; validation, R.A.; data curation, R.A.; writing—original draft preparation, P.S.; writing—review and editing, P.S.; supervision, R.A. All authors have read and agreed to the published version of the manuscript.

Funding: This research received no specific grant from any funding agency in the public, commercial, or not-for-profit sectors.

Data Availability Statement: The datasets generated during the current study are available from the corresponding author on reasonable request.

Conflicts of Interest: The authors declare no conflict of interest.

References

1. Kelly, J.E. Generation IV International Forum: A decade of progress through international cooperation. *Prog. Nucl. Energy* **2014**, *77*, 240–246. [[CrossRef](#)]
2. Dulera, I.V.; Sinha, R.K. High temperature reactor. *J. Nucl. Mater.* **2008**, *383*, 183–188. [[CrossRef](#)]
3. Rubbia, C.; Aleixandre, J.; Andriamonje, S. *A European Roadmap for Developing Accelerator Driven Systems (ADS) for Nuclear Incineration*; The European Technical Working Group: Lungotevere Thacon di Revel, Italy, 2001; ISBN 88-8286-008-6.
4. Arkhipov, V. *Future Nuclear Energy Systems: Generating Electricity, Burning Wastes*; International Atomic Energy Agency: Vienna, Austria, 2007.
5. OECD-NEA. *Accelerator-Driven Systems (ADS) and Fast Reactors (FR) in Advanced Nuclear Fuel Cycles—A Comparative Study*; NEA-3109; Nuclear Energy Agency, Organization for Economic Cooperation and Development: Paris, France, 2002.
6. Bauer, G.S.; Dai, Y.; Maloy, S.Y.; Mansur, L.K.; Ullmaier, H. Summary of the Fourth International Workshop on Spallation Materials Technology (IWSMT-4). *J. Nucl. Mater.* **2001**, *296*, 321–325. [[CrossRef](#)]
7. Gabriel, T.A. The National Spallation Neutron Source Target Station. In *Proceedings of the Topical Meeting on Nuclear Applications of Accelerator Technology*, Albuquerque, NM, USA, 16–20 November 1997.
8. Gromov, B.F. *Heavy Liquid-Metal Coolants in the Nuclear Technologies. Collection of the Conference Reports in Two Volumes*; SSC RF-IPPE: Obninsk, Russia, 1999; Volume 1.
9. Zhang, J.; Li, N. *Review of Studies on Fundamental Issues in LBE Corrosion*; LA-UR-04-0869; Los Alamos National Laboratory: Los Alamos, NM, USA, 2004.
10. Li, N. Active control of oxygen in molten lead–bismuth eutectic systems to prevent steel corrosion and coolant contamination. *J. Nucl. Mater.* **2002**, *300*, 73–81. [[CrossRef](#)]
11. Bardes, B.P. (Ed.) *Properties and Selection: Non-Ferrous Alloys and Pure Metals, Metals Handbook*; American Society for Metals: Materials Park, OH, USA, 1979; Volume 2.
12. Zhang, J. A review of steel corrosion by liquid lead and lead–bismuth. *Corros. Sci.* **2009**, *51*, 1207–1227. [[CrossRef](#)]
13. Cathcart, J.V.; Manly, W.D. *The Mass-Transfer Properties of Various Metals and Alloys in Liquid Lead*; Oak Ridge National Laboratory Technical Report, ORNL-2009; Oak Ridge National Laboratory: Oak Ridge, TN, USA, 1956.
14. Mueller, G.; Heinzl, A.; Schumacher, G.; Weisenburger, A. Control of oxygen concentration in liquid lead and lead–bismuth. *J. Nucl. Mater.* **2003**, *321*, 256–262. [[CrossRef](#)]
15. Benamati, G.; Gessi, A.; Zhang, P.Z. Corrosion experiments in flowing L B E at 450°. *J. Nucl. Mater.* **2006**, *356*, 198–202. [[CrossRef](#)]

16. Ballinger, R.G.; Lim, J.; Li, N. The development and production of functionally graded composite cladding and structural materials for lead-bismuth service. *Trans. Am. Nucl. Soc.* **2006**, *94*, 761.
17. Romano, A.J.; Klamut, C.J.; Gurinski, D.H. *The Investigation of Container Materials for Bi and Pb Alloys. Part I. Thermal Convection Loops*; Brookhaven National Laboratory Technical Report, BNL 811(T-313); Brookhaven National Laboratory: Upton, NY, USA, 1963.
18. Schroer, C.; Wedemeyer, O.; Novotny, J.; Skrypnik, A.; Konys, J. Selective leaching of nickel and chromium from Type 316 austenitic steel in oxygen containing lead–bismuth eutectic (LBE). *Corros. Sci.* **2014**, *84*, 113–124. [[CrossRef](#)]
19. Jing, L. Stress Corrosion Behavior of T91 and 316L Steels in Liquid Lead-Bismuth Eutectic. Ph.D. Thesis, University of Science and Technology of China, Hefei, China, 2015.
20. Gao, Y.; Takahashi, M.; Nomura, M. Experimental study on diffusion of Ni in Lead bismuth eutectic (LBE). *Energy Procedia* **2015**, *71*, 313–319. [[CrossRef](#)]
21. Gorynin, I.V.; Karzov, G.P.; Markov, V.G.; Lavrukhin, V.S.; Yakovlev, V.Y. Structural materials for power plants with heavy liquid metals as coolants. In *Heavy Liquid Metal Coolants in Nuclear Technology (HLMC-98)*; SSC RF-IPPE: Obninsk, Russia, 1998; Volume 1, pp. 120–132.
22. Yachmenev, G.S.; Rusanov, A.E.; Gromov, B.F.; Belomytsev, Y.S.; Skvortsov, N.S.; Demishonkov, A.P. Problems of structural materials corrosion in Lead-Bismuth coolant. In *Heavy Liquid Metal Coolants in Nuclear Technology (HLMC-98)*; SSC RF-IPPE: Obninsk, Russia, 1998; Volume 1, pp. 133–140.
23. Asher, C.; Davies, D.; Beetham, S.A. Compatibility of structural materials with molten lead. *Corros. Sci.* **1977**, *17*, 545–557. [[CrossRef](#)]
24. Muller, G.; Schumacher, G.; Zimmermann, F. Investigation on oxygen controlled liquid lead corrosion of surface treated steels. *J. Nucl. Mater.* **2000**, *278*, 85–95. [[CrossRef](#)]
25. Glasbrenner, H.; Konys, J.; Mueller, G.; Rusanov, A. Corrosion investigations of steels in flowing lead at 400 °C and 550 °C. *J. Nucl. Mater.* **2001**, *296*, 237–242. [[CrossRef](#)]
26. Cathcart, J.V.; Manly, W.D. The mass transfer properties of various metals and alloys in liquid lead. *Corrosion* **1956**, *12*, 43–47. [[CrossRef](#)]
27. Fazio, C.; Sobolev, V.P.; Aerts, A.; Gavrilov, S.; Lambrinou, K.; Schuurmans, P.; Gessi, A.; Agostini, P.; Ciampichetti, A.; Martinelli, L.; et al. *Handbook on Lead-Bismuth Eutectic Alloy and Lead Properties, Materials Compatibility, Thermal-Hydraulics and Technologies*; Organisation for Economic Co-Operation and Development: Paris, France, 2007; ISBN 978-92-64-99002-9.
28. Dinsdale, A.T. SGTE data for pure elements. *Calphad* **1991**, *15*, 317–425. [[CrossRef](#)]
29. TCC. *Thermo-Calc Software User's Guide, Version R*; TCC: Stockholm, Sweden, 2006.
30. Redlich, O.; Kister, A.T. Algebraic representation of thermodynamic properties and the classification of solutions. *Ind. Eng. Chem.* **1948**, *40*, 345–348. [[CrossRef](#)]
31. Boa, D.; Ansara, I. Thermodynamic assessment of the ternary system Bi-In-Pb. *Thermochimi. Acta* **1998**, *314*, 79–83. [[CrossRef](#)]
32. Yoon, S.W.; Lee, H.M. A thermodynamic study of phase equilibria in the Sn-Bi-Pb solder system. *Calphad* **1998**, *22*, 167–178. [[CrossRef](#)]
33. Wojtaszek, Z. Research on intermediate phases in Bi-Pb system. *Zeszyty Nauk. Uni. Jagiell. Ser. Nauk. Mat. Przyrod. Mat. Fiz. Chem.* **1956**, *6*, 151–161.
34. Predel, B.; Schwenmann, W. Analysis of the thermodynamic properties of solid Pb-Bi alloy. *Z. Metallkde.* **1967**, *58*, 553–557.
35. Fon, H.H.; Hanemann, H. Information on lead-Bismuth and lead-antimony-bismuth systems. *Z. Metallkde.* **1940**, *32*, 112–117.
36. Hayasi, M. An X-Ray determination of solid-solubility of Bi in Pb. *Nippon Kinzoku Gakkai-Shi* **1939**, *3*, 123–125.
37. Agarwal, R.; Samui, P.; Jat, R.A.; Singh, Z.; Sen, B.K. Calorimetric investigation of Pb–Bi system. *J. Alloys Compd.* **2010**, *490*, 150–154. [[CrossRef](#)]
38. Agarwal, R.; Samui, P. Enthalpy increment and heat capacity of Pb₃Bi. *J. Alloys Compd.* **2010**, *508*, 333–337. [[CrossRef](#)]
39. Nosek, M.V.; Yan-Sho-Syan, G.V.; Semibrator, N.M. The lead-bismuth phase diagram. *Trudy Inst. Khim. Akad. Nauk. Kaz, USSR* **1967**, *15*, 150–157.
40. Takase, T. Equilibrium diagram of Pb-Bi system. *Nippon Kinzoku Gakkai-Shi* **1937**, *1*, 143–150.
41. Samui, P.; Agarwal, R.; Padhi, A.; Kulkarni, S.G. Thermodynamic investigations of Bi-Ni system Part-I. *J. Chem. Therm.* **2013**, *57*, 470–476. [[CrossRef](#)]
42. Agarwal, R.; Samui, P.; Kulkarni, S.G. Thermodynamic investigations of Bi-Ni system Part-II. *J. Chem. Therm.* **2013**, *57*, 476–484. [[CrossRef](#)]
43. Vassilev, G.P.; Liu, X.J.; Ishida, K. Experimental studies and thermodynamic optimization of the Ni-Bi system. *J. Phase Equil. Diffusion* **2005**, *26*, 161–168. [[CrossRef](#)]
44. Voss, G. Die Legierungen: Nickel-Zinn, Nickel-Blei, Nickel-Thallium, Nickel-Wismut, Nickel-Chrom, Nickel-Magnesium, Nickel-Zink und Nickel-Cadmium. *Z. Anorg. Chem.* **1908**, *57*, 52–58. (In German) [[CrossRef](#)]
45. Seo, S.K.; Cho, M.G.; Lee, H.M. Thermodynamic assessment of the Ni-Bi binary system and phase equilibria of the Sn-Bi-Ni ternary system. *J. El. Mat.* **2007**, *36*, 1536–1544. [[CrossRef](#)]
46. Portevin, M.A. The alloys of nickel and bismuth. *Rev. Metall.* **1908**, *5*, 110–120. [[CrossRef](#)]
47. Predel, B.; Ruge, H. Bildungsenthalpien und bindingsverhältnisse in einigen intermetallischen verbindungen vom NiAs-Typ. *Thermochim. Acta* **1972**, *3*, 411–418. [[CrossRef](#)]
48. Vassilev, G.P.; Lilova, K.I. Notes on some supposed transitions of the phase NiBi. *Cryst. Res. Technol.* **2009**, *44*, 25–30. [[CrossRef](#)]

49. Ghosh, G. Thermodynamic modeling of the nickel-lead-tin system. *Metall. Mater. Trans. A* **1999**, *30*, 1481–1494. [[CrossRef](#)]
50. Alden, T.; Stevenson, D.A.; Wulff, J. Solubility of Nickel and Chromium in Molten Lead. *J. Trans. Metall. Soc. AIME* **1958**, *212*, 15–17.
51. Fleischer, B.; Elliot, J.F. The solubility of iron-nickel alloys in liquid lead:700 °C to 1100 °C, In proceeding of the physical chemistry of metallic solutions and intermetallics compounds. *Natl. Phys. Lab.* **1959**, *1*, 2–12.
52. Miller, K.O.; Elliot, J.F. Phase relationships in the systems Fe-Pb-Ni, Fe-Ni-C(sat) and Fe-Pb-Ni-C,1300 to 1550 °C. *Trans. Metall. Soc. AIME* **1960**, *218*, 900–910.
53. Cavanaugh, C.R.; Elliot, J.F. The activity of nickel in liquid Pb-Ni alloys (700–1000 °C). *Trans. Metall. Soc. AIME* **1964**, *230*, 633–638.
54. International Atomic Energy Agency. *Comparative Assessment of Thermophysical and Thermohydraulic Characteristics of Lead, Lead-Bismuth and Sodium Coolants for Fast Reactors*; IAEA-TECDOC-1289; IAEA: Vienna, Austria, 2002.
55. Martynov, P.N.; Ivanov, K.D. *Properties of Lead–Bismuth Coolant and Perspectives of Non-Electric Applications of Lead-Bismuth Reactor*; IAEA-TECDOC-1056; IAEA: Vienna, Austria, 1997; pp. 177–184.
56. Weeks, J.R. Liquid Metal Compatibility of Structural Materials with Liquid Lead bismuth and Mercury. In Proceedings of the 1997 TMS Annual Meeting, Orlando, FL, USA, 9–13 February 1997.
57. Zhang, J.; Li, N. Review of the studies on fundamental issues in LBE corrosion. *J. Nucl. Mater.* **2008**, *373*, 351–377. [[CrossRef](#)]
58. Gossé, S. Thermodynamic assessment of solubility and activity of iron, chromium, and nickel in lead bismuth eutectic. *J. Nucl. Mater.* **2014**, *449*, 122–131. [[CrossRef](#)]